Case Study

Performance of Atlas GNSS Global Correction Service for High-Accuracy Positioning

Luca Tavasci, Ph.D.[1]; Enrica Vecchi[2]; and Stefano Gandolfi, Ph.D.[3]

Abstract: In the last decade, a number of correction services for global navigation satellite systems (GNSS) precise positioning have been developed, mainly for offshore applications, based on a precise point positioning (PPP) real-time processing. These allow receiving corrections without the need for an internet connection or reference benchmarks around the survey area. In the paper, we tested the Atlas correction service implemented in a Stonex S900A machine (Monza, Italy), with the purpose to verify its performances under optimal operational conditions and in the practical case of a land survey on several benchmarks along the Adriatic coast. The data analysis focused on: accuracy with respect to the reference frame, repeatability of the coordinates considering short and long acquisition periods, time to initialize the survey, and reliability of the formal errors provided by the instrument. The system confirmed the declared performances in most cases and is shown to be a viable alternative to other GNSS techniques also for land surveys where no obstacles affect the sky visibility. **DOI: 10.1061/(ASCE)SU.1943-5428.0000372.** *This work is made available under the terms of the Creative Commons Attribution 4.0 International license, https://creativecommons.org/licenses/by/4.0/.*

Introduction

To date, the use of global navigation satellite systems (GNSS) allows a number of applications for both technical and scientific contexts. Several techniques enable all users to measure three-dimensional coordinates with different associated precisions. For technical applications, real-time kinematic (RTK) (Wang 1999; Langley 1998) and network-RTK (NRTK) (Hofmann-Wellenhof et al. 2007; Cina et al. 2014) modes have become a standard and can be very useful because they provide centimetric precisions in real time, but they both require the availability of ground-based infrastructures (geodetic networks) for the corrections definition and for their transfer to users (radio or internet). Especially in the offshore or mountain areas, RTK and NRTK can be affected by several problems, such as the lack of internet coverage or control points. Moreover, in vast nonurbanized areas, the implementation of a dense geodetic network for positioning could become uneconomical.

A first attempt to overcome the need for ground-based infrastructures and provide corrections for GNSS positioning has been done implementing satellite-based augmentation systems (SBAS), which provide coverage of wider areas and broadcast GNSS corrections to a large number of users through the use of geostationary satellites coupled with a continuously operating reference stations (CORS) network for the corrections estimation (Li et al. 2020; Walter et al. 2010; Choy et al. 2017; Wang et al. 2018). Several countries have implemented their public SBAS based on code-observables corrections. Earlier examples are the US wide area augmentation system (WAAS) and the European geostationary navigation overlay system (EGNOS), but several other services are now available or under development as reported in the map in GSA (2020a, p. 14) or their table (GSA 2020a, p. 97). However, these services typically use code observables and provide only a metric precision, which fails to achieve the centimeter-level positioning accuracy necessary for most demanding technical applications.

The last 10 years have seen the development and the spread of several global services for real-time positioning with centimeter level precision as well as acquisition of phase corrections (Anantakarn and Witchayangkoon 2019). These commercial services, mainly developed for offshore applications, use the precise point positioning (PPP) approach (Bisnath and Gao 2009; Kouba and Heroux 2001; Zumberge et al. 1997), supported by the computing of corrections from global CORS networks. The use of permanent stations of known coordinates allows modeling of spatial-correlated source of errors and defining a correction model suitable in the area covered by the GNSS network. These corrections can be finally sent to users from geostationary satellites through L-band signals (Rizos et al. 2012; Gumilar et al. 2019). These augmentation systems deliver corrections for accurate positioning to wide areas with theoretical precisions a little lower than the ones of NRTK, maintaining errors in the order of a few centimeters (Anantakarn and Witchayangkoon 2019; Hemisphere 2020). Using these services, it is possible to obtain a homogeneous positioning quality using a single receiver also without the need of an internet connection (Choy et al. 2017; Boylan 2016). Nevertheless, signals from commercial SBAS services cannot be implemented by all the GNSS receivers because it is necessary to have specific hardware and purchase a subscription (Choy et al. 2017).

Currently, different companies provide similar positioning services, a list of which has been given in table format by GSA (2020a, p. 98) together with the declared accuracies and the used constellations. For some of those, it is also possible to receive corrections via internet connection. Moreover, the European Union is developing an open service, also based on PPP corrections, for the Galileo

[1]Postdoctoral Research Fellow, Dept. of Civil Chemical Environmental and Material Engineering, Univ. of Bologna, Viale Risorgimento 2, Bologna 40136, Italy. ORCID: https://orcid.org/0000-0003-0395-7185. Email: luca.tavasci@unibo.it

[2]Ph.D. Candidate, Dept. of Civil Chemical Environmental and Material Engineering, Univ. of Bologna, Viale Risorgimento 2, Bologna 40136, Italy (corresponding author). ORCID: https://orcid.org/0000-0002-6524-9216. Email: enrica.vecchi@unibo.it

[3]Full Professor, Dept. of Civil Chemical Environmental and Material Engineering, Univ. of Bologna, Viale Risorgimento 2, Bologna 40136, Italy. Email: stefano.gandolfi@unibo.it

Note. This manuscript was submitted on December 21, 2020; approved on June 3, 2021; published online on August 13, 2021. Discussion period open until January 13, 2022; separate discussions must be submitted for individual papers. This paper is part of the ***Journal of Surveying Engineering***, © ASCE, ISSN 0733-9453.

constellation, named the High Accuracy Service (HAS), which should provide real-time accuracies smaller than 20 and 40 cm (95%) for the horizontal and vertical components, respectively, promising a convergence time shorter than 300 s for the global service and 100 s over the European area (GSA 2020b). In this case, corrections will be sent to users directly by GNSS satellites using the Galileo E6b band or by internet, without the use of geostationary satellites. The service will be fully operational after 2025. Furthermore, also the Chinese BeiDou is about to implement a high-accuracy correction service based on PPP in its BeiDou satellite based augmentation system (BDSBAS) (BeiDou 2019), which should provide horizontal accuracies within 30 cm and vertical accuracies within 60 cm at 95%, with convergence time shorter than 30 min.

All these correction services are roughly similar in their functioning principle, providing slightly different accuracies and different spatial coverages, regional or global. In this paper, we will focus on the Atlas service managed by Hemisphere GNSS. This infrastructure is composed of 200 permanent stations distributed on a global scale, and it provides corrections for global positioning system (GPS), global navigation satellite system (GLONASS), Galileo, and BeiDou constellations, allowing a submeter positioning accuracy. Three geostationary satellites cover almost all the Earth, thus making Atlas solutions very flexible. The Atlas correction service is available on single- and dual-frequency GNSS receivers at three different levels:

- Atlas Basic: 50 cm 95% [30-cm root mean square (RMS)],
- H30: 30 cm 95% (15-cm RMS), and
- H10: 8 cm 95% (4-cm RMS).

In general, the precision related to each level of the service can be reached only after a period of convergence, which is declared to be 10–30 min depending on the selected service.

The aim of this paper is to assess the performance of the Atlas correction system in the best operating conditions, meaning the absence of obstacles to sky visibility, that could occur at midlatitudes (about 45° north) where the elevation of the geostationary satellite is quite low (about 30°). Furthermore, a test was carried out in order to verify if this technology can actually be an effective alternative to the classical RTK technique in case of land applications. The analysis was possible thanks to the availability of a Stonex S900A receiver (Monza, Italy), which implements the Atlas service for the standalone positioning. This receiver can track all carrier signals sent by the modern GNSS satellites (GPS, GLONASS, BeiDou, and Galileo) using 600 channels, with a frequency up to 20 Hz. It integrates a high-accuracy antenna together with an internal multipath suppressive board. A subscription is needed to benefit from the full Atlas service, allowing one to receive L-band corrections without any time restrictions.

Different aspects have been investigated: the convergence time needed for the measures to initialize, the congruence with the declared reference system, the measures' repeatability, and the reliability of the formal error estimated in real time. Data have been acquired in two different contexts, one representing ideal conditions of sky visibility and with long sessions on a fixed point, and the other concerning a real survey located along the Adriatic coast. In both cases, the same analysis approach has been followed, and the corresponding results have been compared in order to evaluate the impact of the environmental conditions.

Data Sets

Two different data sets were acquired for testing the Atlas performance in different contexts, both following the idea to record 1-Hz solutions on a reference point for a time span long enough to allow a statistical analysis of the solutions. In particular, the first data set was acquired in ideal conditions and for a sufficient time span in order to assess the performance of the system. In the following sections, we will refer to this data set as the lab test.

Differently, a second data set, hereafter called the field test, was acquired in order to verify which performance can be expected in certain operational conditions. In particular, we used as reference some benchmarks belonging to an already existing geodetic network along the Adriatic coast. The location of all the test benchmarks is shown in Fig. 1. The same S900A receiver was used for all the acquisitions acquiring all the available constellations.

For the GNSS constellations, at the test time (2019), besides the 32 GPS satellites and the 23 GLONASS ones, about 24 and 10 satellites were actually available for the Galileo and BeiDou constellations, respectively. These have been improving in the last years, and thus the number of satellites available is now higher.

Lab Test

The first data set consists of 135 h of GNSS data acquired in June 2019 over the roof of the Engineering Department of the University of Bologna at the sampling frequency of 1 Hz, thus providing a representative statistical sample for a general assessment about the Atlas global correction service during a standalone positioning. The absence of significant obstacles that could obstruct the proper satellites view from the receiver guaranteed ideal conditions. Data were acquired using all the available constellations in 41 sessions with a time span ranging from about 1–5 h. The receiver was switched off and restarted after each session with the aim to simulate a number of surveys in the most similar conditions and allowing a statistical evaluation of the convergence time the system needs to provide the declared performances. The upper-bound limit of about 5 h was not a choice but a technical limit of the instrument controller coupled with the S900A, which was not designed for acquiring autonomously real-time positions for very long sessions. Moreover, in some cases, we shortened the observing sessions to obtain a higher number of new converging phases and better evaluate this parameter. Once the instrument had converged, the acquisition continued in order to evaluate repeatability of the solutions, also on long acquisition times.

In three cases, the raw GNSS observables (codes and phases) were recorded too, in order to calculate the postelaborated coordinates with a PPP approach by using GIPSY-OASIS II version 6.4 software. This was done by continuously acquiring data for about 12 h because the record of raw data does not undergo the limitations occurring to Atlas real-time solutions, and it allowed us to have a reference position for the chosen point.

Field Test

The second data set was acquired during September 2019 to consider the heterogeneous conditions of a real situation. In this case, the surveyed test points were those of the Coastal Geodetic Network (RGC), realized in 2016 thanks to the collaboration between the Coastal Monitoring Unit of regional agency for prevention, environment and energy of emilia-romagna (ARPAE) and the Department of Civil, Chemical and Environmental Engineering (DICAM) of the University of Bologna (Vecchi et al. 2020). These benchmarks, located along the Adriatic coast, are used for local monitoring surveys and their coordinates are aligned to the official national reference system ETRS89-ETRF2000 (2008.0 epoch) (Gandolfi et al. 2017a; Vecchi et al. 2020). RGC monographs available on the ARPAE Cartographic Portal (ARPAE 2021), have been used as a reference for the following analysis. These measures involved 15 RGC benchmarks, and for each one, a 10-min-long

Fig. 1. Location of the chosen benchmarks in Emilia-Romagna region: for the lab test (triangle) and field test (circles). Coordinates are latitude and longitude expressed in WGS84 reference system. (Base map © OpenStreetMap contributors.)

observing session was performed acquiring data at a 1-Hz frequency. Also in this case, signals of all the constellations were used.

The campaign involved three distinct days, surveying five points each. The time spent between the instrument turn on and when it reached converged condition (CONV marked on the screen) was accounted for, but no data were acquired in the meanwhile. Moving from a point to another, the receiver was not powered off in order to avoid new initializations of the system, in the perspective of a time optimization required by operational conditions. In several cases, the convergence was lost when moving, and the time necessary to reach it again was accounted for after having reached the next RGC benchmark. In only one case (RICE0300), it was impossible to perform the Atlas positioning because of an obstruction of the sky visibility in the direction of the geostationary satellite.

Methods

On the basis of the described data sets, the following analysis has been performed to evaluate different aspects:

- accuracy: the coherence between the Atlas coordinates and the reference positions,
- convergence time: the time needed by the system to work at the declared accuracy,
- repeatability/precision: the inherent agreement between coordinates obtained by measuring the same point after a certain time span, and
- reliability of the formal errors: the representativity of the formal horizontal and vertical errors [horizontal root mean square (HRMS)/vertical root mean square (VRMS)] value compared with the real errors.

Henceforth, RMS will refer to the instrument formal errors because the interface uses HRMS/VRMS to indicate the a priori estimation of the positioning errors. Differently, the sample standard deviation (STD) will denote the sample standard deviation calculated a posteriori in the coordinate analysis.

Accuracy

Assessment of the Atlas system's accuracy required a set of reference coordinates expressed in the same reference system stated by Hemisphere, which is the ITRF2008. By comparing these reference coordinates with the ones obtained by the survey, it is possible to describe the agreement of the observed values with their true values. In order to compute the most representative ITRF2008 coordinates of the lab test benchmark estimated using the Atlas service, we averaged the values of all the coordinates acquired under the condition of having a formal horizontal error (HRMS) less than 4 cm. Because the system is declared converged when the HRMS goes under 8 cm, this should allow us to consider only positions recorded in best operating conditions. The number of such positions actually used was 254,376, meaning more than 70 h of observations.

The reference position for the same point was estimated by computing three different PPP solutions using the GIPSY-OASIS II software [developed by jet propulsion laboratory (JPL)]. These solutions were calculated starting from raw data acquired during long observing sessions (about 12 h), and they should guarantee an accuracy within 1 cm (Gandolfi et al. 2017b). The formal reference frame to which the PPP solutions are aligned is IGb08, a coherent update of the ITRF2008, therefore fully comparable with the Atlas reference. The three independent PPP solutions were averaged, obtaining the reference position with which to compare the one

estimated using Atlas. The comparison between the postprocessed PPP coordinates and the ones obtained from Atlas is given in Table 1, where positions are expressed in the universal transverse mercator (UTM) system. The agreement of the mean Atlas position with the reference one (IGb08) is at the centimeter level, thus proving the correct realization of the Atlas reference system. In light of this, the averaged Atlas coordinates will be used a reference for all the following evaluations.

As for the field test, the reference coordinates of each benchmark were compared with the averaged value of the coordinates surveyed in the related 10-min session performed using Atlas in converged conditions. Because the RGC reference coordinates are expressed in the ETRF2000 (2008.0)-UTM32 frame, a transformation was performed to align the Atlas solutions and allow the comparison. In order to compare coherently the field test results with those of lab test, for the latter, we also evaluated the accuracy by considering the mean coordinates recorded in the first 10 min after convergence for each of the 41 sessions.

Convergence Time

The evaluation of the convergence time of the solutions is a very significant aspect, especially for the practical point of view, because it is the time that a surveyor has to wait before starting to work, and it could depend on several elements, such as the satellites view and the multipath effect (Seepersad and Bisnath 2015; Abou Galala et al. 2018). When the receiver is turned on, the system needs some time to provide the declared precision. The used H10 service fixes a threshold of 8 cm for the HRMS value to consider a solution as converged. The controller displays a mark CONV to state the converged status of the system, and a surveyor should use this information to start operating expecting the performance declared by Hemisphere. The manufacturers declare a convergence time ranging from 10 to 40 min (Hemisphere 2020). Because all the solutions with a HRMS value equal or smaller to 8 cm are considered as converged, we computed the time necessary to reach this condition for each measuring session.

Repeatability

Coordinate repeatability is the parameter that can be used to evaluate the positioning precision. It refers to the agreement between results obtained by measuring the same point in the same conditions in relation to a certain range of time. In the analysis, we distinguish between two different concepts: precision and pass-to-pass repeatability.

Precision has been evaluated by computing the STD of the coordinates acquired during the same session in converged conditions. This evaluation followed the same procedure for both the data sets, with sessions of different length: a few hours for the lab test and 10 min for the field test. The precision aspect can be analyzed in deeper detail by observing the histogram showing the distribution of the residuals, or in other words the probability of occurrence of a certain value. The histogram of the horizontal residuals was obtained by considering the Euclidean distance of the coordinates with respect to the real value, choosing classes of 0.5 cm. The histogram of the height residuals have been defined using classes of 1 cm. Both the described graphs have been obtained by considering only the residuals related to converged solutions for all the acquired sessions.

The pass-to-pass repeatability has been defined for agricultural applications (ISO 2012; Hemisphere 2018), and it represents the capability of the system to provide coherent coordinates within a short time range. Therefore, we simulated a test comparing each couple of observations spaced out by 15 min to obtain a distribution of these biases. We calculated their standard deviation, which actually represents the pass-to-pass precision, and the maximum bias between these couples of coordinates. The declared pass-to-pass repeatability for the Atlas service is about 2.5 cm (1σ) (Hemisphere 2018).

Another analysis focused on the precision, which could be obtained from static surveys with different acquisition times (1, 5, 10, 15, and 30 min). The result of a static survey is typically the average value of the coordinates acquired during the observing session; therefore, we used moving averages to simulate several of these surveys. The STD of the time series of averaged coordinates was computed to define the precision of the measuring sessions performed using different time spans. This computation concerned only the time series with at least 90 min of data in converged conditions, and the standard deviation has been calculated for each time duration.

Reliability of Formal Errors

During a real-time positioning, users can have feedback on the coordinate quality thanks to two statistical parameters: the formal horizontal and vertical errors (HRMS and VRMS). Therefore, these values should be reliable to avoid accepting solutions that are actually less precise or waiting too long to record the coordinates. In particular, the formal error should be reliable, especially after reaching the convergence; otherwise, the user might not realize they were working without the expected precision.

The lab test allowed the evaluation of the reliability of the formal errors, thanks to the availability of a reference position to calculate the real errors of the coordinates. For each of the 41 sessions, a time series of the residuals between Atlas coordinates and the reference position was calculated. The value of each residual has been compared with its related formal error, expressed in terms of RMS (σ), multiplied by a scalar n in order to define a certain confidence level.

A reliability parameter ν_k^i was calculated for any epoch i by using

$$\nu_k^i = |P_k^{\text{ref}} - P_k^i| > n \times \text{RMS}^i \tag{1}$$

where $k = N$, E, and h components; P_k^{ref} = reference coordinates; and P_k^i = measured ones. The formal error RMS is the HRMS in case of northing and easting, whereas it is the VRMS for the height. We used $n = 2$ to define the 95% confidence level or $n = 3$ for the 99.73% one. If the absolute value of the residual is higher than the threshold ($n \times \text{RMS}^i$) this means that the formal error has been underestimated at the considered confidence level. The percentages of solutions affected by an underestimation of the formal error have been evaluated through

$$\text{Rej}_{k,\%} = \sum_i \frac{\nu_k^i}{n_k} \tag{2}$$

where n_k = number of observations of the session used to weight the value.

Results

Accuracy

Lab Test

Once verifying the overall consistency of the reference frame used for Atlas correction with the declared ITRF2008 by analyzing long time series (Table 1), we evaluated the level of accuracy achievable with shorter acquisition periods, which could be more suitable in technical applications. Table 2 presents, for each session, the biases

Table 1. Reference UTM coordinates obtained from the PPP elaboration

Kind of solution	N (m)	E (m)	h (m)
GIPSY PPP	4,928,689.894	685,273.766	139.931
Atlas	4,928,689.883	685,273.760	139.925
Difference	−0.011	−0.006	−0.006

Note: Data are the average of three independent solutions using GIPSY-OASIS II software, averaged value of Atlas coordinates with associated HRMS lower than 4 cm, and difference between the two sets of coordinates. Northing (N); and Easting (E)

Table 2. Differences between averaged Atlas coordinates computed considering the first 10 min after the convergence and the reference ones (Table 1) for each measuring session

Session	dN (m)	dE (m)	dh (m)
1	0.024	0.018	0.012
2	0.016	0.100	0.084
3	0.016	0.142	0.072
4	0.008	0.086	0.129
5	0.011	0.027	0.113
6	0.021	0.076	0.111
7	0.074	0.061	0.159
8	0.037	0.166	0.181
9	0.014	0.033	0.048
10	0.080	0.079	0.131
11	0.013	0.071	0.034
12	0.033	0.018	0.150
13	0.016	0.076	0.143
14	0.007	0.018	0.250
15	0.011	0.085	0.038
16	0.041	0.173	0.031
17	0.059	0.047	0.090
18	0.164	0.438	0.278
19	0.023	0.070	0.055
20	0.009	0.033	0.033
21	0.019	0.023	0.115
22	0.043	0.300	0.052
23	0.027	0.025	0.010
24	0.043	0.032	0.113
25	0.010	0.060	0.080
26	0.034	0.015	0.018
27	0.010	0.008	0.047
28	0.027	0.126	0.061
29	0.042	0.451	0.255
30	0.166	0.099	0.037
31	0.036	0.037	0.021
32	0.036	0.108	0.068
33	0.031	0.041	0.019
34	0.010	0.007	0.030
35	0.012	0.034	0.042
36	0.027	0.035	0.051
37	0.009	0.005	0.047
38	0.027	0.068	0.099
39	0.089	0.080	0.107
Average	0.035	0.086	0.088

Note: dN = discard along the northing direction; dE = discard along the easting direction; and dh = discard along the up direction.

between the averaged coordinates obtained during the first 10 min after reaching the convergence and the reference position. Values are related to a topocentric reference system. The obtained accuracies are about 3 cm for the northing and about 9 cm for the easting and the height. Nevertheless, nine sessions have associated biases higher than 10 cm concerning plan components, and the same is verified in 14 cases considering the height component.

Table 3. Differences between Atlas coordinates averaged on 10 min and the study ones for each RGC point

Site	dN (m)	dE (m)	dh (m)
PCPG0020	0.269	0.276	0.027
PCPG0100	0.022	0.049	0.023
PCPG0200	0.071	0.031	0.208
PCPG0300	0.136	0.131	0.077
PCPG0400	0.030	0.051	0.187
SAPC0700	0.025	0.070	0.031
SAPC0650	0.043	0.051	0.060
SAPC0600	0.049	0.219	0.423
SAPC0500	0.015	0.098	0.010
SAPC0400	0.038	0.074	0.077
RICE0400	0.096	0.068	0.036
RICE0500	0.226	1.037	0.112
RICE0550	0.074	0.063	0.147
RICE0700	0.055	0.009	0.157
Average	0.071	0.091	0.113

Therefore, the best accuracy is not always reachable within the first 10 min of acquisition in converged conditions.

Field Test

The differences between the average Atlas coordinates obtained on the RGC benchmarks and their reference values are given in Table 3. The average accuracy is within 9 cm for the plan components, whereas it is about 11 cm for the height. Because the RICE0500 biases are significantly higher with respect to the others, probably due to the poor visibility in the geostationary satellite direction, they were excluded in the computation of the average values. On a total of 14 sessions, in four cases, the biases are higher than 10 cm concerning the plan components, and the same is verified in six cases for the height. This test confirmed that the acquisition in the first 10 min after the convergence may be affected by significant biases.

Convergence Time

Lab Test

The time periods needed to reach the convergence after the switching on the instrument are shown in Fig. 2 for the 41 sessions. Fig. 2 also shows the variation of the HRMS over time. It can be observed that the formal error rapidly decreases during the first 10 min, and then it tends to stabilize around 8 cm. The average convergence time is 31 min even though a strong variability can be noticed. In fact, despite the same boundary conditions, the convergence time varies from 18 to 48 min. In terms of STD the dispersion of these values is about 8 cm.

Field Test

In the field test, the instrument has been maintained as always switched on during the transfer from a point to the next one, with the purpose of verifying if it is possible to work in different areas without waiting for the whole convergence period each time. In only two cases, the L-band signal has been acquired continuously and the system was found already in converged condition once reached a new benchmark of the RGC. In the remaining 12 cases, the convergence time was considered to be the period between the instrument setup and reaching new convergence. This could be in some cases the same that could have been found by restarting the instrument. The average convergence time we observed in the field test is about 22 min, with an actually range between 13 and 29 min.

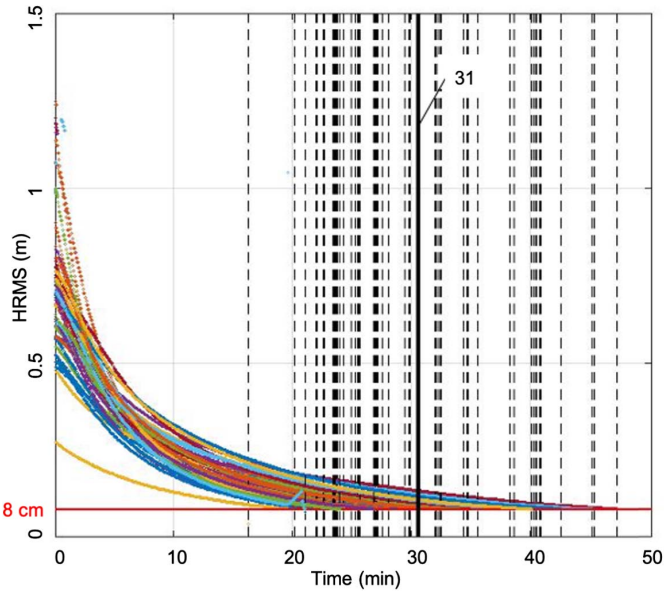

Fig. 2. HRMS trend (curves) and convergence times (dotted lines) of 41 sessions. The average convergence time is shown with the thick solid line. Only solutions with HRMS higher than 8 cm are plotted.

Repeatability

The analysis of the repeatability focused on three different possible scenarios: measures repeated after long periods, measures acquired within a short time range, and static surveys. Fig. 3 provides an example of a 4.5-h time series, which could be useful to understand the behavior of the Atlas positioning over time. The time series shows the residuals with respect to a topocentric reference system

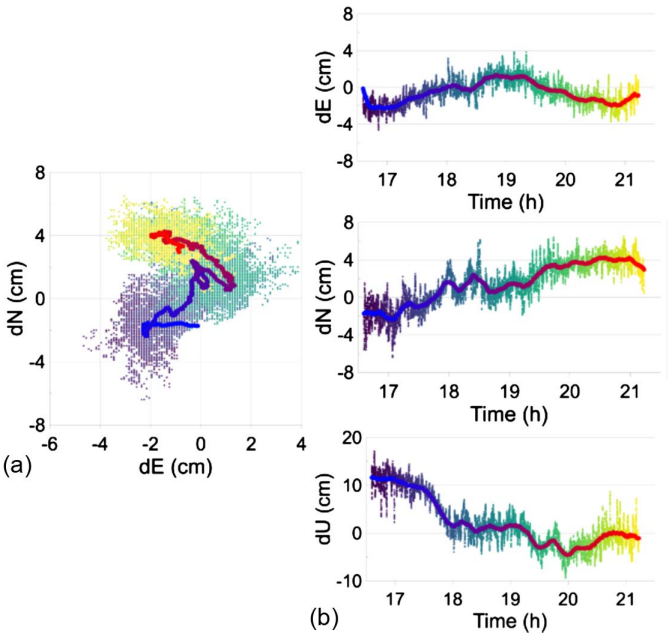

Fig. 3. Example of time series of the residuals with respect to the reference position: (a) plan components; and (b) time series of the three components (east, north, and up) separately. The thick line represents data filtered by a moving average (900 epochs), and the shades are used to express the evolution over time.

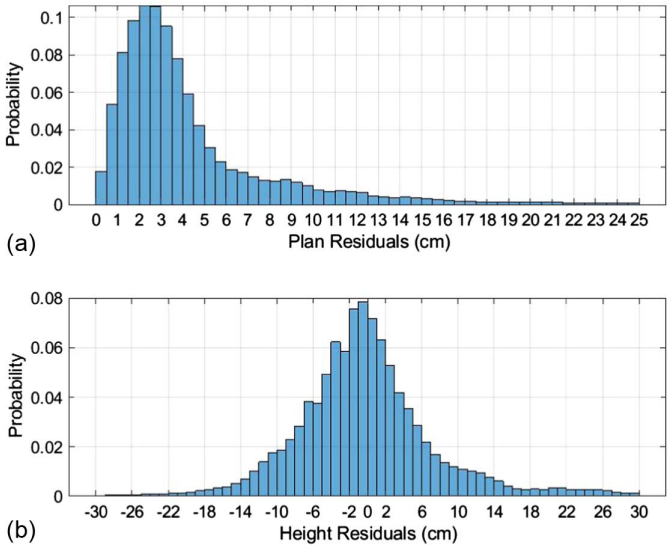

Fig. 4. Histograms of the lab test residuals: (a) horizontal residuals; and (b) height component.

centered on the reference position. The thick lines represent data filtered by a moving average.

In Fig. 3(a), the residuals of the plan components are represented, and different shades are used to represent their time variation. Looking at the whole data set, coordinates seem to be grouped around the reference value. Nevertheless, by filtering the time series using a simple moving average (thick line), a drift over time can be observed. This is probably due to tidal effects or tropospheric delays that are not completely modeled, maybe because of coarse density of the ground network used to compute Atlas corrections. Consequently, if we focus on short time spans, coordinates are scattered around the local mean, which is less than what they were around the mean over the whole period. This can be easily observed in the north–east graph reported in Fig. 3 for the plan components, but the same can be said as for the Up component by looking at its time series.

Precision

Fig. 4 shows the histogram of all the horizontal [Fig. 4(a)] and the height [Fig. 4(b)] residuals recorded under converged conditions in the lab test. As for the plan, the residuals with the higher probability range between 2 and 3 cm, and the probability to obtain errors higher than 8 cm is about the 87%, which is a little lower than the declared 95%.

Table 4 reports the standard deviations of the coordinates for both data sets, averaged for all the sessions. Concerning the lab test, because the measuring sessions were longer than the ones of the field test, we also analyzed the values obtained in the same conditions, thus considering only the first 10 min after reaching the convergence.

Table 4. Standard deviations of the coordinates acquired in convergent conditions for all the solutions of the lab test, first 10 min of the lab test, and the field test

Considered test	RMS N (m)	RMS E (m)	RMS h (m)
Lab test	0.031	0.068	0.086
Lab test, 10 min	0.015	0.024	0.023
Field test	0.013	0.020	0.030

In terms of standard deviations, the precisions related to the 10 min of observations are higher than the ones related to longer sessions. This could be explained looking at the behavior previously shown in Fig. 3. Moreover, the northing seems to be more precise with respect to the other components. The field test provided results compliant with those obtained in the lab test, with STD between about 1 and 3 cm.

Table 5. Precisions of static surveys simulated through moving averages expressed in terms of RMS

Acquisition time	RMS N (m)	RMS E (m)	RMS h (m)
1 s	0.016	0.026	0.031
1 min	0.015	0.025	0.027
5 min	0.015	0.024	0.023
10 min	0.015	0.024	0.023
15 min	0.015	0.024	0.022
30 min	0.014	0.022	0.021

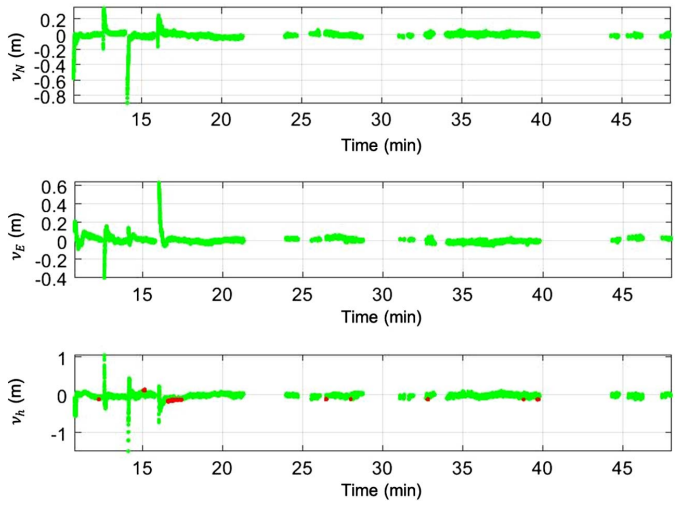

Fig. 5. Example of a time series providing optimal results. The x-axis refers to the time, expressed in minutes; the y-axis refers to residual values of northing, easting, and height. Light points represent reliable estimations of the formal errors, and dark points indicate residuals that are higher than expected according to 2σ confidence interval.

Pass-to-Pass Repeatability

Atlas pass-to-pass repeatability is represented by the value of the standard deviation of couple of coordinates spaced out of 15 min. Therefore, this analysis was carried out only for the lab test. The STD of the pass-to-pass precision computed for all available data are 1.9, 2.7, and 5.0 cm for the northing, easting, and height components, respectively. Results concerning the plan components are consistent with the pass-to-pass precision declared for the service (2.5 cm). Nevertheless, in some cases, the pass-to-pass residuals could reach higher values, which are around 10 cm and may rise up to 30 cm in the worst cases. Furthermore, comparing the pass-to-pass repeatability with the precision discussed previously, we can confirm that Atlas solutions tend to drift over long periods, whereas they tend to be closer within short intervals.

Precision of Static Surveys

The precisions of static surveys simulated through moving averages are reported in Table 5 in terms of STD of the coordinates, depending on the considered acquisition time. Even when increasing the acquisition time, the solution precision does not take significant advantages, especially for the plan components. Moving from 1 to 30 min, the increase in precision is about 1–3 mm for northing and easting, whereas for the height component it is about 6 mm. Focusing on the height, benefits related to longer acquisition times are consistent especially ranging from 1 s to 5 min. The fact that within the range of 30 min, the precision does not take advantage of longer acquisition times is probably due to the instability over long period of the Atlas solution.

Reliability of the Formal Errors

Figs. 5 and 6 represent two examples of time series of the residuals in northing, easting, and height. A light shade is used when the real error is smaller than n times the formal error according to Eq. (1), and a dark shade is used to highlight cases of underestimations. In particular, Fig. 5 relates to a session acquired in favorable conditions, which provided optimal results, whereas Fig. 6 shows an example of time series related to a session affected by some anomalies. In the

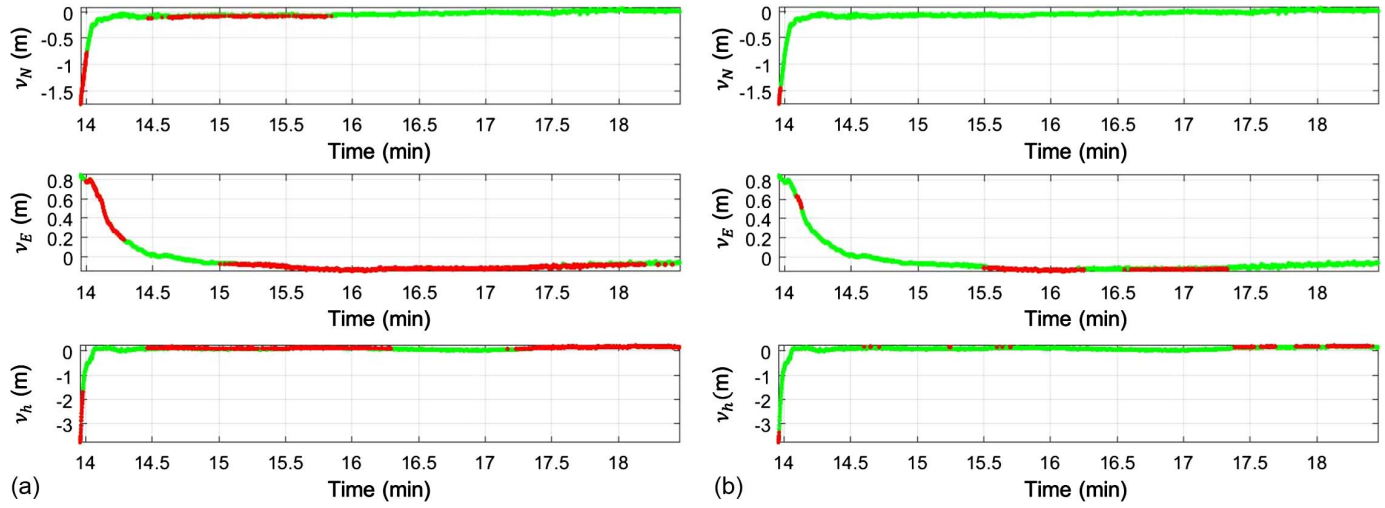

Fig. 6. Example of a time series showing anomalous behavior of the formal errors: (a) 2σ confidence interval; and (b) 3σ confidene interval. The x-axis refers to the time, expressed in minutes; the y-axis refers to residual values of northing, easting, and height. Light points represent reliable estimations of the formal errors, and dark points indicate residuals that are higher than expected.

J. Surv. Eng., 2021, 147(4): 05021005

Table 6. Percentages of convergent solutions affected by underestimation of the formal errors, considering a 2σ confidence interval for all the sessions, only sessions with optimal results, and all sessions considering a 3σ confidence interval

Confidence interval	N (%)	E (%)	h (%)
2σ, all sessions	1.96	9.34	9.92
2σ, optimal sessions	0.59	1.33	3.42
3σ, all sessions	0.45	4.31	4.11

latter case, Fig. 6(a) was obtained by considering 2σ confidence interval, and Fig. 6(b) relates to 3σ.

Basing on Eq. (2), the average percentages of solutions for which the associated HRMS or VRMS value are underestimated were computed for all data sessions and are reported in Table 6. Considering the 2σ confidence interval, the formal error is reliable for the northing, with only the 2% of the solutions affected by underestimation of the formal error. Differently, for the easting and the height, the underestimations of the HRMS and VRMS occur in 9% and 10% of the cases, respectively. These values are higher than the 5% expected for the defined confidence interval. In Table 6, the first line refers to all the data, including some sessions for which anomalous percentages of underestimated errors were found (11 sessions out of a total of 41). Excluding these sessions from the statistics, the results are presented in the second line of Table 6. In this case, the formal errors are compliant with the expected probabilities for all coordinate components. Furthermore, the same evaluations have been done for all data considering a 3σ confidence interval, and the results are given in Line 3 of Table 6. Also in this case, the percentages of underestimated formal errors are higher than the expected significance level.

Conclusions

The aim of the proposed study is to analyze Atlas global correction service, examining its performance in standalone positioning conditions. Several tests have been performed using a S900A Stonex receiver in two different contexts. A first data set consists of repeated measures on a fixed point located on the rooftop of the Engineering Department of the University of Bologna, and the second one involved 15 different points belonging to the RGC of Emilia Romagna. In both cases, we simulated a situation where there is no availability of network coverage for NRTK corrections or benchmarks for RTK positioning. These conditions are usual in offshore surveying or in remote areas outside of NRTK network boundaries. Several time series of 1-Hz solutions were acquired and used to evaluate different parameters: accuracy, convergence time, reliability of the formal errors, coordinate precision, and repeatability.

Atlas reference frame has shown to be coherent with what the company declares (ITRF2008) at the centimeter level. This was assessed by comparing Atlas solutions to a reference position estimated using GIPSY software and the same GNSS observables. Considering the first 10 min after the convergence of the solutions, the positioning accuracy is about 8–10 cm in the plan, with some value up to several decimeters, in both lab conditions and the field surveying.

A significant aspect from the practical point of view concerns the convergence time that is required before starting the survey. In the lab test, the convergence time was assessed after restarting the instrument at the beginning of each session, and its average value is about 31 min, characterized by a large variability (18–48 min). On the other hand, in the field test, the average convergence time is about 22 min, obtained by operating without switching off the instrument but losing the converges conditions because of the transfers from one point to another.

We evaluated the reliability of the formal errors (HRMS and VRMS) displayed by the instrument, which should provide an estimation of the positioning precision, helping users to be aware of the survey quality in real time. An underestimation of these errors may lead the users to accept solutions that are not complying the survey standards. Therefore, we checked the percentage of cases in which this could occur. Considering a 95% confidence level, the formal errors have shown to be reliable for the northing, whereas they result in underestimated values in about the 10% of the cases for easting and height components. Similar results were found considering 3σ confidence interval. Nevertheless, by excluding some anomalous sessions from the statistics, the formal errors were found fully reliable for all the coordinate components.

As for the precision, the lab test showed that the 87% of the solutions are distributed within 8 cm in the plan, a percentage slightly lower than the declared 95%. In terms of STD, the coordinates acquire an overall precision of about 3.1, 6.8, and 8.6 cm considering the northing, easting, and height components, respectively. On the other hand, the system provides better precisions considering short time spans: in terms of pass-to-pass (measures spaced by 15 min in time) the STD values are 2.0, 2.6, and 4.7, whereas considering 1-Hz acquisition over 10 min, the precision values become 1.5, 2.4, and 2.3. Finally, we investigated the possibility to improve the precision by acquiring data with static sessions, testing time spans ranging from 1 to 30 min. Using Atlas, differently from other techniques, the precision is not significantly improved by performing static positioning. This fact can be interpreted as a consequence of the slow drift occurring to the position solutions over time, which is shown in Fig. 3.

Despite the fact that 2019 data have been considered for this work, we are confident that the increased number of available satellites does not change dramatically the system performances and this contribution can be a reliable picture of the Atlas functioning at the time. Furthermore, it will be a benchmark for evaluations on the progresses of the technique in the future, when both Galileo and BeiDou will be fully operational and implemented in the updated Atlas network. Summarizing, the coordinates obtained using the Atlas correction system are well aligned to the ITRF2008 reference frame and can be considered accurate at the 10-cm level in the plan when the system reaches convergence, with only few exceptions. For coordinates measured within a short period (10–20 min), the service provides precisions at the 2–3 cm level, whereas the difference between coordinates measured after long periods may be over 10 cm in a significant percentage of cases.

From the practical point of view, the viability of the Atlas positioning in land surveys is strongly affected by the presence of obstacles to the sky visibility, especially in the direction of the geostationary satellite that sends the corrections. On the other hand, compared with other GNSS techniques, the Atlas positioning is independent of the presence of a stable internet connection, and it provides just slightly poorer accuracies. The time required by the system to start the survey is still much higher for the Atlas with respect to a classical network RTK. Therefore, the tested technology can be suitable for land surveys where the presence of obstacles to the sky visibility is minimal and the system does not require being frequently reinitialized.

Data Availability Statement

The processing code used during the study is available online in accordance with funder data retention policies (https://gipsy-oasis.jpl.nasa.gov). All data that support the findings of this study are available from the corresponding author upon reasonable request.

Acknowledgments

Special thanks go to Stonex Srl, which provided the GNSS instrument and careful assistance.

References

Abou Galala, M., M. R. Kaloop, M. M. Rabah, and Z. M. Zeidan. 2018. "Improving precise point positioning convergence time through TEQC multipath linear combination." *J. Surv. Eng.* 144 (2): 04018002. https://doi.org/10.1061/(ASCE)SU.1943-5428.0000250.

Anantakarn, K., and B. Witchayangkoon. 2019. "Accuracy assessment of L-band Atlas GNSS system in Thailand." *Int. Trans. J. Eng. Manage. Appl. Sci. Technol.* 10 (1): 91–98.

ARPAE (Regional Agency for Prevention, Environment and Energy of Emilia-Romagna). 2021. "ER visore cartografico." Accessed May 1, 2021. https://servizigis.arpae.it/Html5Viewer/index.html?viewer=Geoportal.Geoportal.

BeiDou. 2019. "The application service architecture of BeiDou navigation satellite system." Accessed May 1, 2021. http://en.beidou.gov.cn/SYSTEMS/Officialdocument/202001/P020200116328218237495.pdf.

Bisnath, S., and Y. Gao. 2009. "Current state of precise point positioning and future prospects and limitations." In *Observing our changing Earth*, 615–623. Berlin: Springer.

Boylan, R. 2016. *An evaluation of the performance of two different global satellite navigation systems, Trimble's CenterPoint RTX and a conventional network RTK system*, 1–14. Toowoomba, Australia: Univ. of Southern Queensland.

Choy, S., J. Kuckartz, A. G. Dempster, C. Rizos, and M. Higgins. 2017. "GNSS satellite-based augmentation systems for Australia." *GPS Solutions* 21 (3): 835–848. https://doi.org/10.1007/s10291-016-0569-2.

Cina, A., P. Dabove, A. M. Manzino, and M. Piras. 2014. "Augmented positioning with CORSs network services using GNSS mass-market receivers." In *Proc., 2014 IEEE/ION Position, Location and Navigation Symp.-PLANS 2014*, 359–366. New York: IEEE.

Gandolfi, S., N. De Nigris, M. Morelli, L. Tavasci, L. Poluzzi, and N. Cenni. 2017a. "La rete geodetica costiera della regione emilia-romagna." In *Proc., ASITA 2017*, 599–604. New York: Springer.

Gandolfi, S., L. Tavasci, and L. Poluzzi. 2017b. "Study on GPS–PPP precision for short observation sessions." *GPS Solutions* 21 (3): 887–896. https://doi.org/10.1007/s10291-016-0575-4.

GSA (European GNSS Agency). 2020a. "GNSS user technology report." Accessed May 1, 2021. https://www.euspa.europa.eu/simplecount_pdf/tracker?file=uploads/technology_report_2020.pdf.

GSA (European GNSS Agency). 2020b. "Galileo high accuracy service (HAS)." Accessed May 1, 2021. https://www.gsc-europa.eu/sites/default/files/sites/all/files/Galileo_HAS_Info_Note.pdf.

Gumilar, I., B. Bramanto, T. P. Sidiq, and B. Mulyadi. 2019. "Assessment of different real time precise point positioning correction over the sea area." *KnE Eng.* 4 (3): 115–123. https://doi.org/10.18502/keg.v4i3.5836.

Hemisphere. 2018. "Hemisphere GNSS whitepaper." Accessed May 1, 2021. https://www.hemispheregnss.com/wp-content/uploads/2018/12/hemispheregnss_atlas_whitepaper_20181119.pdf.

Hemisphere. 2020. "Atlas GNSS global correction service." Accessed December 12, 2020. https://www.hemispheregnss.com/product/atlas-gnss-global-correction-service/.

Hofmann-Wellenhof, B., H. Lichtenegger, and E. Wasle. 2007. *GNSS–global navigation satellite systems: GPS, GLONASS, Galileo, and more*. New York: Springer.

ISO. 2012. *Tractors and machinery for agriculture and forestry—Test procedures for positioning and guidance systems in agriculture—Part 2: Testing of satellite-based auto-guidance systems during straight and level travel*. ISO 12188-2:2012. Geneva: ISO.

Kouba, J., and P. Heroux. 2001. "Precise point positioning using IGS orbit and clock products." *GPS Solutions* 5 (2): 12–28. https://doi.org/10.1007/PL00012883.

Langley, R. B. 1998. "RTK GPS." *GPS World* 9 (9): 70–76.

Li, R., S. Zheng, E. Wang, J. Chen, S. Feng, D. Wang, and L. Dai. 2020. "Advances in BeiDou navigation satellite system (BDS) and satellite navigation augmentation technologies." *Satell. Navig.* 1 (1): 1–23. https://doi.org/10.1186/s43020-020-00010-2.

Rizos, C., V. Janssen, C. Roberts, and T. Grinter. 2012. "*Precise point positioning: Is the era of differential GNSS positioning drawing to an end?*" In *Proc. of FIG Working Week 2012*, 6–10. Rome: Precise Point Positioning.

Seepersad, G., and S. Bisnath. 2015. "Reduction of PPP convergence period through pseudorange multipath and noise mitigation." *GPS Solutions* 19 (3): 369–379. https://doi.org/10.1007/s10291-014-0395-3.

Vecchi, E., M. Aguzzi, C. Albertazzi, N. De Nigris, S. Gandolfi, M. Morelli, and L. Tavasci. 2020. "Third beach nourishment project with submarine sands along Emilia-Romagna's coast: Geomatic methods and first monitoring's results." *Rend. Lincei Sci. Fis. Nat.* 31 (1): 79–88. https://doi.org/10.1007/s12210-020-00879-w.

Walter, T., J. Blanch, and P. Enge. 2010. "Coverage improvement for dual frequency SBAS." In *Proc., 2010 Int. Technical Meeting of the Institute of Navigation*, 344–353. San Diego: Stanford Univ.

Wang, J. 1999. "Stochastic modeling for real-time kinematic GPS/GLONASS positioning." *Navigation* 46 (4): 297–305. https://doi.org/10.1002/j.2161-4296.1999.tb02416.x.

Wang, L., et al. 2018. "Initial assessment of the LEO based navigation signal augmentation system from Luojia-1A satellite." *Sensors* 18 (11): 3919. https://doi.org/10.3390/s18113919.

Zumberge, J. F., M. B. Heflin, D. C. Jefferson, M. M. Watkins, and F. H. Webb. 1997. "Precise point positioning for the efficient and robust analysis of GPS data from large networks." *J. Geophys. Res.* 102 (B3): 5005–5017. https://doi.org/10.1029/96JB03860.